EPJ Web of Conferences **218**, 03002 (2019) https://doi.org/10.1051/epjconf/201921803002
PhiPsi 2017

Recent Results on Meson Decays from A2

Patrik Adlarson for the A2 Collaboration[1,⋆]

[1] *Institut für Kernphysik, Johannes Gutenberg-Universität Mainz, D-55099 Mainz, Germany*

Abstract. Light meson decays are used to investigate topics related to fundamental aspects of particle physics. Precision measurements of meson Dalitz decays give input to theoretical evaluations of the Hadronic Light-by-Light contribution (HLbL) to the anomalous magnetic moment of the muon. The A2 collaboration, using the Crystal Ball/TAPS setup at MAMI, has recently published several high precision results on transition form factors which are related to HLbL. Pseudoscalar η' decays allow for studies of topics like $\pi\pi$ scattering lengths, effective field theories and fundamental symmetries. In 2014 the collaboration had a dedicated experimental campaign with one of its main goals to measure the dynamics of $\eta' \to \pi^0\pi^0\eta$ with high precision. A brief overview of the experimental setup, physics motivations, analyses and results are given.

1 Introduction

Mesons and their properties continue to be of interest to the hadron and particle-physics communities. The electromagnetic transition form factors (TFF) are of interest for probing the precision frontier of the Standard Model (SM) and for understanding the intrinsic properties of the hadrons themselves. There has been a renewed interest in light meson TFFs of e.g. π^0, η and ω, as they provide input to theoretical contributions to the anomalous magnetic moment of the muon, $(g-2)_\mu$. Also the η' meson and its decay modes play an important role in our understanding of Quantum ChromoDynamics (QCD) and its related phenomenological models. This proceeding will focus on four recent results from the A2 collaboration: the Dalitz decays $\pi^0 \to e^+e^-\gamma$ [1], $\eta \to e^+e^-\gamma$, $\omega \to \pi^0e^+e^-$ [2], and the decay $\eta' \to \pi^0\pi^0\eta$ [3]. The proceeding structure is as follows: after the introduction (section 1) a description of the Crystal Ball-TAPS experimental setup at MAMI is given (section 2), followed by the three physics channels related to the TFFs and the $\eta' \to \pi^0\pi^0\eta$ channel (sections 3 and 4, respectively). Finally, a summary is given (section 5).

2 Experimental Setup

The electron accelerator MAMI (Mainz Microtron) [4, 5] can provide an electron beam up to 1.604 GeV. The Pseudoscalar (P= π^0, η, η') and Vector (V=ω) mesons are produced in the reaction $\gamma p \to P/Vp$ when beam photons impinge on an extended Liquid Hydrogen target. The photon beam is created when the electron beam interacts with a radiator, producing bremsstrahlung electrons and photons. The postbremsstrahlung electrons are detected to provide the energy measurement of

⋆e-mail: padlarso@uni-mainz.de

the photon beam which are incident on the target. For energies covering ~0.08-1.5 GeV the Glasgow-Mainz tagger is used [6–8], while for higher photon energies the end-point tagging spectrometer (EPT) [9] is used. The final state $e^{\pm}$- and γ-particles from the meson decays were measured in the Crystal Ball (CB) [10] and TAPS [11, 12] calorimeters. The CB detector consists of 672 NaI(Tl) crystals forming a sphere encapsulating the target, covering 93% of 4π. The target is covered by the Particle Identification Detector (PID) [13] used to identify charged particles. The TAPS detector is installed 1.5 m downstream and consists of 384 hexagonal BaF_2 crystals. To be able to run with higher beam currents, e.g. in the η' production experiment, 18 of the BaF2 crystals closest to the beam line were replaced with 72 $PbWO_4$ crystals. The results presented here were analysed with data taken between the years 2007-2014.

3 Transition Form Factors

3.1 Motivation: a_μ and Meson TFF

One of the most precisely known quantities in the SM is that of the anomalous magnetic moment of the muon, $a_\mu = (g_\mu - 2)/2$. The muon magnetic moment, measured by the E821 experiment, is known experimentally to the 10th decimal [14] with even more precise measurements planned in the near future [15, 16]. The E821 result deviates from the SM calculation by 3-4σ [17, 18]. Theoretically, the poorest understood SM contributions to a_μ are from interactions involving hadrons, $a_\mu^{hadr} = a_\mu^{HVP} + a_\mu^{HLbL}$, where a_μ^{HVP} and a_μ^{HLbL}, refer to the hadronic vacuum polarization (HVP) and Hadronic Light-by-Light (HLbL), respectively. The latter contribution has historically been difficult to estimate as it was mostly obtained from models suffering from large and uncontrolled uncertainties [19]. In recent years dispersive approaches have been proposed to reduce the present day errors of HLbL [20, 21]. A better understanding of HLbL comes from the study of meson TFFs [22]. Meson TFFs can be accessed in kinematical regions of four-momentum transfer q^2 through study of both space- and time-like processes. The A2 collaboration can measure the TFFs in the time-like region by measuring pseudoscalar Dalitz decays, i.e. $P \to \gamma^*\gamma \to e^+e^-\gamma$, but also $\omega \to \pi^0 e^+e^-$. For the case $P \to \gamma\gamma^*$, the q^2 range is given by $4m_l^2 < q^2 < m_P^2$. In general, however, $A \to B\gamma^*$ has the range $m_l^2 \leq q^2 \leq (m_A - m_B)^2$, $(l = e, \mu)$. The time-like meson TFFs $F_P(m_{ll})$ and $F_{\omega\pi^0}(m_{ll})$ are obtained by dividing the differential decay distribution with its corresponding Quantum ElectroDynamics (QED) contribution. In the Vector Meson Dominance model (VMD), the virtual photon couples to an intermediate virtual-vector-meson state (e.g. $V = \rho, \omega, \phi$). To quantify the TFF dependence the slope parameter a_P is defined, which reflects the slope value extracted at $q^2 = 0$. Related to this quantity is also the effective mass Λ, which, under the VMD approximation, parametrizes the TFFs in a pole approximation. These are given by

$$a_P \equiv \frac{F_P(m_{ll})}{dq^2}|_{q=0}, \quad F_{P\gamma/\omega\pi^0}(m_{ll}) = (1 - \frac{m_{ll}^2}{\Lambda^2})^{-1}, \; \Lambda^{-2} = a_P. \tag{1}$$

Due to the smallness of the momentum-transfer range for the π^0 Dalitz decay, the form factor is parametrized as $F_{\pi^0\gamma}(m_{ll}) = 1 + a_\pi \cdot (m_{ll}/m_{\pi^0})^2$.

3.2 $\pi^0 \to e^+e^-\gamma$

The PDG value of the slope parameter for the π^0 Dalitz decay, $a_{\pi^0} = 0.032 \pm 0.004$ [23], is dominated by the CELLO result, $a_{\pi^0} = 0.0326 \pm 0.0026_{\text{stat}} \pm 0.0026_{\text{syst}}$ [24]. The CELLO result introduces a model dependence. This is because a_{π^0} is extrapolated from relatively large momentum transfers in the space-like region and assuming the validity of VMD. It makes sense for a direct measurement

of the slope parameter in the time-like region, which can be provided by the A2 collaboration. The most accurate theoretical descriptions of a_{π^0} are obtained from Padé approximants [26] and dispersive theory [27]. The π^0 Dalitz decay was searched for in events containing 3 and 4 reconstructed clusters. For the final event selection kinematic-fit [28, 29] was used both to select the signal and reject the main background contribution, coming from $\pi^0 \to \gamma\gamma$ events. The lepton pairs were identified by requiring two hits in the PID. The final event sample of $4.0 \cdot 10^5$ π^0 Dalitz decays was split up into 18 bins in the $m(e^+e^-)$ range 15-120 MeV. The Dalitz decays were corrected for the efficiency in each bin of $m(e^+e^-)$ and divided by the corresponding QED contributions and decay widths. The form factor squared, $|F_{\pi^0\gamma}|^2$, shown as a function of $m(e^+e^-)$ for the π^0 Dalitz decay, is seen in the left frame of Fig. 1. By fitting the pole approximation its slope parameter was obtained as $a_\pi = 0.030 \pm 0.010_{\text{tot}}$, where the error includes both statistical and systematical uncertainties. This result is in good agreement with the PDG value [23] and theoretical estimates [26, 27]. At the same time as the A2 result became available [1], also the NA62 collaboration released their results [25]. They obtained the value $a_\pi = 0.0368 \pm 0.0051_{\text{stat}} \pm 0.0025_{\text{syst}}$ which is in good agreement with the A2 result. In the near future a new high-statistics π^0 Dalitz decay measurement from A2 is planned.

3.3 $\eta \to e^+e^-\gamma$

For the η Dalitz decay, the best experimental result for the slope parameter comes from the NA60 collaboration, $\Lambda_{\eta\gamma}^{-2} = (1.934 \pm 0.067_{\text{stat}} \pm 0.050_{\text{syst}})$ GeV^{-2} [30]. There are two previous results from the A2 collaboration at MAMI [32, 33] and the higher-statistics result measured the value $\Lambda_\eta^{-2} = (1.95 \pm 0.15_{\text{stat}} \pm 0.10_{\text{syst}})$ GeV^{-2}. A recent theoretical prediction comes from the Jülich group, using a dispersive approach [34, 35]. In addition, there are also predictions based on Padé approximants [36] and with a chiral Lagrangian approach [37]. For the Dalitz decay analysis both 3- and 4-cluster events were selected, and kinematic-fit was used both to identify the signal channel and reject background contributions. The only serious background candidate comes from $\eta \to \gamma\gamma$ where one photon undergoes conversion in the material between the production vertex and the calorimeter material. The remaining final event sample contained $5.4 \cdot 10^4$ η Dalitz decays and the fit with the pole approximation to the data gives $\Lambda_\eta^{-2} = (1.97 \pm 0.13)$ GeV^{-2}, in agreement with the previous results [30–33] and theoretical calculations [34–37].

3.4 $\omega \to e^+e^-\pi^0$

Much attention has been given to the time-like $\omega\pi^0$ TFF in the q-range covered by the $\omega \to \pi^0 l^+ l^+$ decay. This is because the available experimental data from NA60 [30, 31] and Lepton-G [38] for $m(l^+l^-) > 600$ MeV are discrepant, so far, with every available theoretical approach. One of these approaches are also calculated under model-independent assumptions [39]. The experimental data are, however, in agreement with each other. For the A2 analysis only five-cluster events were selected, as four-cluster events resulted in much larger background contributions. For this channel there are three major sources of background: $\gamma p \to \pi^0\pi^0 p$, $\gamma p \to \pi^0\eta p$ and $\omega \to \pi^+\pi^-\pi^0$. Suppression of these channels required analysis of energy losses in the PID, cuts on the kinematic-fit confidence level (CL), vertex cuts and cuts based on electromagnetic shower properties. The number of $\omega \to \pi^0 e^+e^-$ events in the final sample was $1.1 \cdot 10^3$. The fit to the form factor $|F_{\omega\pi^0}|^2$, shown in the right frame of Fig. 1, gives the fit value $\Lambda_{\omega\pi^0}^{-2} = (1.99 \pm 0.21_{\text{tot}})$ GeV^{-2}. This is a bit lower compared to the latest result from NA60, $\Lambda_{\omega\pi^0}^{-2} = (2.223 \pm 0.026_{\text{stat}} \pm 0.037_{\text{syst}})$ GeV^{-2} [30], and in better agreement with theoretical calculations. A firm conclusion may not be drawn, however, as the accuracy of the data points at large $m(e^+e^-)$ is not sufficient.

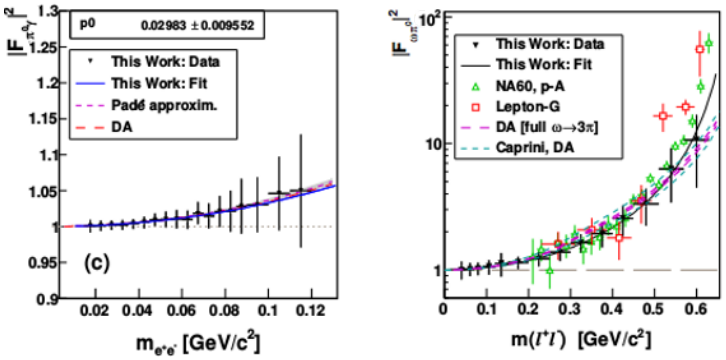

Figure 1. (left) $|F_{\pi^0\gamma}|^2$ results with total uncertainties. The fitted values to the points are shown by blue lines, with $p0$ being the slope parameter a_π. Comparison to calculations with Padé approximants [26] is seen as the short-dashed magenta line with a gray error band and to the dispersive analysis (DA) [27] shown as the red, long-dashed line. The error band for the latter analysis is by a factor of four narrower, compared [26], and is omitted. (right) $|F_{\omega\pi^0}(m_{e^+e^-})|^2$ results (black filled triangles) fitted with the pole approximation (black solid line). The experimental results from Lepton-G [38] (open red squares) and NA60 in p–A collisions [30] (open green triangles) are shown together with dispersive analysis calculation by the Bonn group [40] (magenta dashed lines) and upper and lower bounds by Caprini [41] (cyan dashed lines) for the discontinuity calculated with the partial-wave amplitude $f_1(t)$ based on [40].

4 $\eta' \to \pi^0\pi^0\eta$

The η' meson and its decay modes play an important role in understanding low-energy QCD and its related theoretical models [42, 46, 47]. The neutral decay mode $\eta' \to \pi^0\pi^0\eta$ allows a test of pion scattering length combinations, most notably seen as a cusp in the $m(\pi^0\pi^0)$ spectrum at the $\pi^+\pi^-$ mass threshold [43]. The matrix element for the $\eta' \to \pi_1\pi_2\eta$ decay is described by the Dalitz plot where three body decays are expressed in terms of the variables X and Y, defined in eqn. (2). The Dalitz plot is expanded around $X = Y = 0$ and a polynomial is used for describing the matrix element,

$$X = \frac{\sqrt{3}}{Q}(T_{\pi_1} - T_{\pi_2}), \quad Y = \frac{T_\eta}{Q}(\frac{m_\eta}{m_\pi} + 2) - 1, \quad |M|^2 \sim 1 + aY + bY^2 + cX + dX^2, \tag{2}$$

where a, b, c and d are Dalitz plot parameters. The observables T_{π_1}, T_{π_2} and T_η are the kinetic energies of the two final-state pions and η, respectively. All kinetic energies are calculated in the η' rest frame. The sum of kinetic energies are given by $Q = T_\eta + T_{\pi_1} + T_{\pi_2} = m_{\eta'} - m_\eta - 2m_\pi$. All Dalitz plot parameters of odd-powered X are expected to be 0 for symmetry reasons. Recent experimental determinations and theoretical estimates of the Dalitz plot parameters are given in Table 1. The reaction $\gamma p \to \eta' p \to \pi^0\pi^0\eta p \to 6\gamma p$ was searched for in 7-cluster events, assuming that one of the clusters was from the recoil proton. Suppression of the background channel $\gamma p \to \pi^0\pi^0\pi^0 p$ was done by testing the corresponding kinematic-fit hypothesis and applying CL selection criteria. The final event sample still contained non-peaking background distributions. In order to estimate the signal content in the Dalitz plot, the data were distributed into different regions of X and Y. For each region a polynomial of fourth order together with the MC η' signal line shape was fitted to the data. The Dalitz plot parameter values, given in Table 1 were based on $1.2 \cdot 10^5$ events. Besides the A2 result [3] there are two recent high statistics samples on the neutral decay mode, measured by the GAMS-4π [48] and

Experiment $\eta' \to \pi^0\pi^0\eta$	***a***	***b***	***d***
A2 [3]	-0.074(8)(6)	-0.063(14)(5)	-0.050(9)(5)
BESIII [49]	-0.087(9)(6)	-0.073(14)(5)	-0.074(9)(4)
GAMS4π [48]	-0.067(16)(4)	-0.064(29)(5)	-0.067(20)(3)
Theory $\eta' \to \pi\pi\eta$			
Large-Nc [42]	-0.098(48)	-0.050(1)	-0.092(8)
RChT [42]	-0.098(48)	-0.033(1)	-0.072(8)
U(3) Ch.EFT ($\eta' \to \pi^0\pi^0\eta$) [46]	-0.123	-0.104	-0.047

Table 1. Dalitz plot-parameter values for $\eta' \to \pi^0\pi^0\eta$ with errors given in the parentheses. For the experimental data, the first and second parentheses denote the statistical and systematical errors, respectively.

the BESIII collaborations [49]. The A2 result is consistent with these measurements. In addition, for the first time the statistics and experimental resolution allowed, an observation of a structure below the $\pi^+\pi^-$ mass threshold, in good agreement with the predicted cusp based on the $\pi\pi$ scattering length combination, $a_0 - a_2$, previously extracted from $K \to 3\pi$ decays [50].

5 Summary

In these proceedings, three recent results from the A2 collaboration were presented for the TFFs $|F_{\pi^0\gamma}|$, $|F_{\eta\gamma}|$ and $|F_{\omega\pi^0}|$. These were obtained by analyzing the decays $\pi^0 \to e^+e^-\gamma$, $\eta \to e^+e^-\gamma$ and $\omega \to \pi^0e^+e^-$ and the slope parameters for the e/m TFFs were given. While the results for the π^0 and η Dalitz decays are in agreement with other experimental results and theoretical calculations, $|F_{\omega\pi^0}|$ are in a better agreement with theoretical calculations, compared to the available experimental data. However, because of limited experimental statistics, no firm conclusion can be drawn to rule out the previous $\omega \to \pi^0l^+l^-$ results. For the decay mode $\eta' \to \pi^0\pi^0\eta$ the Dalitz-plot parameters were given. In the future, results for the decays $\eta' \to e^+e^-\gamma$ and $\eta' \to \omega\gamma$ from A2 can be expected.

References

[1] P. Adlarson *et al.* **(A2 Collaboration at MAMI)**, Phys. Rev. C **95** 025202 (2017).
[2] P. Adlarson *et al.* **(A2 Collaboration at MAMI)**, Phys. Rev. C **95** 035208 (2017).
[3] P. Adlarson *et al.* **(A2 Collaboration at MAMI)**, arXiv:1709.04230 [hep-ex].
[4] H. Herminghaus *et al.*, IEEE Trans. Nucl. Sci. **30**, 3274 (1983).
[5] K.-H. Kaiser *et al.*, Nucl. Instrum. Methods Phys. Res. A **593**, 159 (2008).
[6] I. Anthony *et al.*, Nucl. Instrum. Methods Phys. Res. A **301**, 230 (1991).
[7] S. J. Hall *et al.*, Nucl. Instrum. Methods Phys. Res. A **368**, 698 (1996).
[8] J. C. McGeorge *et al.*, EPJ A **37**, 129 (2008).
[9] P. Adlarson *et al.*, Phys. Rev. C 92, 024617 (2015).
[10] A. Starostin *et al.*, Phys. Rev. C **64**, 055205 (2001).
[11] R. Novotny, IEEE Trans. Nucl. Sci. **38**, 379 (1991).
[12] A. R. Gabler *et al.*, Nucl. Instrum. Methods Phys. Res. A **346**, 168 (1994).
[13] D. Watts, *Proceedings of the 11th International Conference on Calorimetry in Particle Physics*, Perugia, Italy, 2004 (World Scientific, Singapore, 2005), p. 560.
[14] G. W. Bennett, *et al.* **(The g-2 Collaboration)**, Phys. Rev. D **73**, 072003 (2006).

[15] J. Grange *et al.* **(Muon g-2 Collaboration)**, FERMILAB-FN-0992-E, FERMILAB- DESIGN-2014-02; B. L. Roberts, these proceedings.
[16] T. Mibe **(J-PARC g-2 Collaboration)**, Chin. Phys. C **34**, 745 (2010); these proceedings.
[17] M. Davier, A. Hoecker, B. Malaescu, Z. Zhang. EPJ C **71**, 1515 (2011).
[18] M. Benayoun, P. David, L. DelBuono, F. Jegerlehner, EPJ C **75**, 613 (2015).
[19] A. Nyffeler, Phys. Rev. D **94**, 053006 (2016).
[20] V. Pauk, M. Vanderhaeghen, Phys. Rev. D **90**, 113012 (2014).
[21] G. Colangelo, M. Hoferichter, M. Procura, JHEP 1409, **091** (2014); G. Colangelo, M. Hoferichter, B. Kubis, M. Procura, P. Stoffer, Phys. Lett. B **738**, 6 (2014); G. Colangelo, M. Hoferichter, M. Procura, P. Stoffer, JHEP **1509**, 074 (2015).
[22] L. G. Landsberg, Phys. Rep. **128**, 301 (1985).
[23] C. Patrignani *et al.* **(Particle Data Group)**, Chin. Phys. C **40**, 100001 (2016).
[24] H. J. Behrend *et al.* **(CELLO Collaboration)**, Z. Phys. C **49** (1991) 401 (1991).
[25] C. Lazzeroni *et al.* **(NA62 Collaboration)**, arXiv:1612.08162 [hep-ex].
[26] P. Masjuan, Phys. Rev. D **86**, 094021 (2012).
[27] M. Hoferichter, B. Kubis, S. Leupold, F. Niecknig, S.P. Schneider, EPJ C **74**, 3180 (2014).
[28] V. Blobel, E. Lohrmann. Statistische Methoden der Datenanalyse, Teubner Studienbücher, Teubner, e-book http://www.desy.de/ blobel/eBuch.pdf, 1998.
[29] S. Prakhov *et al.* **(Crystal Ball Collaboration at MAMI and A2 Collaboration)**, Phys. Rev. C **79**, 035204 (2009).
[30] R. Arnaldi *et al.*, Phys. Lett. B **757**, 47 (2016).
[31] R. Arnaldi *et al.*, Phys. Lett. B **677**, 260 (2009).
[32] H. Berghäuser *et al.*, Phys. Lett. B **701**, 562 (2011).
[33] P. Aguar-Bartolome *et al.* Phys. Rev. C **89**, 044608 (2014).
[34] C. Hanhart, A. Kupść, U.-G. Meißner, F. Stollenwerk, A. Wirzba, EPJ C **73**, 2668 (2013); *ibid.* **75**, 242 (2015).
[35] C. W. Xiao, T. Dato, C. Hanhart, B. Kubis, U.-G. Meißner, A. Wirzba, arXiv:1509.02194 [hep-ph].
[36] R. Escribano, P. Masjuan, P. Sanchez-Puertas, Phys. Rev. D **89**, 034014 (2014); EPJ C **75**, 414 (2015).
[37] C. Terschlüsen, Diploma Thesis, University of Gießen, 2010; C. Terschlüsen, S. Leupold, M. F. M. Lutz, EPJ A **48**, 190 (2012).
[38] R. I. Dzhelyadin *et al.*, Phys. Lett. B **102**, 296 (1981).
[39] B. Ananthanarayan, I. Caprini, B. Kubis, EPJ C **74**, 3209 (2014).
[40] S. P. Schneider, B. Kubis, F. Niecknig, Phys. Rev. D **86**, 054013 (2012).
[41] I. Caprini, Phys. Rev. D **92**, 014014 (2015).
[42] R. Escribano, P. Masjuan, J. J. Sanz- Cillero. JHEP, **05**, 094 (2011).
[43] B. Kubis, S P. Schneider, EPJ C **62**, 511 (2009).
[44] N. Beisert, B. Borasoy, Nucl. Phys. A, **716** 186 (2003).
[45] B. Borasoy, R. Nissler, EPJ A, **26** 383 (2005).
[46] B. Borasoy, U.-G. Meissner, R. Nissler, Phys. Lett. B **643**, 41 (2006).
[47] T. Isken, B. Kubis, S. P. Schneider, P. Stoffer, EPJ C **77** 489 (2017).
[48] A. M. Blik *et al.* **(GAMS4π collaboration)**, Phys. Atom. Nucl. **72** 231 (2009).
[49] M. Ablikim *et al.* **(BESIII Collaboration)**, arXiv:1709.04627 [hep-ex].
[50] M. Bissegger, A. Fuhrer, J. Gasser, B. Kubis, A. Rusetsky, Nucl. Phys. B **806**, 178 (2009).